ANALYSIS AND OPTIMAL DESIGN OF PRESTRESSED CONCRETE FOLDED PLATES

by

Govindaswamy Rajasekar

B.S., Indian Institute of Technology
Madras, India, 1976

A MASTER'S THESIS

submitted in partial fulfillment of the

requirements for the degree

MASTER OF SCIENCE

Department of Civil Engineering

KANSAS STATE UNIVERSITY
Manhattan, Kansas

1977

Approved:

Major Professor

TABLE OF CONTENTS

Page

LIST OF FIGURES i

LIST OF TABLES iii

NOTATIONS v

Chapter 1: INTRODUCTION 1

Chapter 2: ANALYSIS OF FOLDED PLATES 5

Chapter 3: APPLICATION EXAMPLES 25

Chapter 4: COMPARISON BETWEEN THE PROPOSED METHOD OF ANALYSIS AND THE BEAM METHOD OF ANALYSIS AND METHOD OF ANALYSIS USING FINITE DIFFERENCE SOLUTIONS 41

Chapter 5: VALIDITY OF THE PRINCIPLE OF SUPERPOSITION 63

Chapter 6: OPTIMAL SELECTION OF PRESTRESSING FORCE AND CABLE SAG 70

CONCLUSIONS 109

ACKNOWLEDGEMENT 110

REFERENCES 111

Appendix A: Principal Stresses and Direction 112

Appendix B: Torsional Moment of Inertia of a Rectangular Cross-Section 115

Appendix C: Source List of the Computer Programs 116

Appendix D: Input-Output Details for the Computer Programs . . . 133

Appendix E: Moment of Inertia and Product of Inertia 141

THIS BOOK CONTAINS NUMEROUS PAGES WITH THE ORIGINAL PRINTING BEING SKEWED DIFFERENTLY FROM THE TOP OF THE PAGE TO THE BOTTOM.

THIS IS AS RECEIVED FROM THE CUSTOMER.

LIST OF FIGURES

Figure		Page
1	Force Resolution at a Ridge of a Folded Plate.	6
2	Structure Cross-Section Showing Relative Joint Displacement	8
3	Distributed Plate Longitudinal Stresses and Deflections.	9
4	Portion of the Cross-Section of a Folded Plate Showing Position of Plates After Deformation	11
5	Wind Force on Buildings (ASCE Committee on Wind Forces).	14
6	Induced Plate Loads Due to Straight or Draped Prestressed Cables	15
7	Primary Longitudinal Stresses in End Plate Due to Direct Prestressing.	17
8	Folded Plate With Edge Beams	19
9	Flow Chart for General Folded Plate Analysis - Main Program	22
10	Flow Chart for General Folded Plate Analysis, Subroutine for Computation of Internal Tractions	24
11	Cross-Section of the Folded Plate Analyzed by Ramaswamy.	26
12	Cross-Section of the Folded Plate Analyzed by Swartz . .	29
13	Coordinate System for Calculation of Principal Stresses.	30
14	Cross-Section Analyzed by Yitzhaki	35
15	Cross-Section Analyzed by Billington	39
16	Coordinate System and Moment Sign Convention for Beam Method of Analysis.	42
17	Analysis of Billington (1) Folded Plate Using Beam Theory.	46
18	Cross-Section of Folded Plate Analyzed by Ramaswamy. . .	48
19	Analysis of Ramaswamy (1) Folded Plate Using Beam Theory.	52

LIST OF FIGURES (Continued)

Figure		Page
20	Typical Sawtooth Folded Plate Cross-Section.	55
21	Cross-Sections of Folded Plates Analyzed in Reference 12	58
22	Variation of σ_x and M_{px} in a Plate	64
23	Possible Cable Geometry in a Typical Plate	77
24	Flow Chart for Prestressed Folded Plate Analysis Only, Main Program	80
25	Cross-Section of Folded Plate Analyzed by J. C. Brough and B. H. Stephens	101

LIST OF TABLES

Table		Page
3.1	Comparison of Computed Results With Those Solutions at Midspan by Ramaswamy.	27
3.2a	Comparison of Computed Results With Those by Swartz. .	31
3.2b	Principal Stresses and Direction	32
3.3a	Comparison of Computed Results With Those by Yitzhaki	37
3.3b	Comparison of Results by Considering the Effect of Torsional Stiffness of Edge Beam With Those When This Effect is Neglected.	37
3.4	Comparison of the Computed Results With Those by Billington	40
4.1	Comparison of Solutions.	59
4.2	Comparison of Computed Results With Those by the Authors of Reference 12.	60
4.3	Comparison of Computed Results With Those by Authors in Reference 12.	61
5.1	Validity of Superposition.	67
6.1.1	Analysis of the Folded Plate for Loading	82
6.1.2	Analysis of Folded Plate for Prestressing (unit force and sag)	82
6.1.3	Simplex Table.	86
6.1.4	Analysis for Load and Optimum Prestressing	88
6.2.1	Analysis for Load.	90
6.2.2	Analysis for Prestressing (unit force and sag)	90
6.2.3	Simplex Table.	97
6.2.4	Stresses at Transfer σ_x psi.	100
6.2.5	Stresses at Final Loads σ_x psi	100
6.4.1	Analysis of the Folded Plate for Load.	103

LIST OF TABLES (Continued)

Table | Page

6.4.2 Analysis of the Folded Plate for Prestressing (unit force and sag). 103

6.4.3 Simplex Table 107

NOTATIONS

c - torsional moment of inertia of the edge beam

c_d - concrete cover

d_n - thickness of a plate

D_n - longitudinal stress at n^{th} ridge due to prestressing only

DP - direct prestress

E_n - eccentricity of the parabolic prestressing cable, measured at midspan from the line joining the two end points of the cable

EP - eccentric prestress

f_{ci} - concrete strength in compression at transfer

f_{ti} - concrete strength in tension at transfer

f_{co} - concrete strength in compression at final load

f_{to} - concrete strength in tension at final load

h_n - plate width

I_n - moment of inertia of the transverse cross-section of the n^{th} plate about an axis passing through the c.g. of that cross-section and in a direction normal to the plane of the plate

J_n - moment of inertia of a unit longitudinal width of the cross-section of n^{th} plate.

K_n - rotation coefficient of n^{th} plate

ℓ - span of the folded plate

$M_{p_{max}}$ - maximum plate moment

M_{px} - plate moment at a distance x from midspan

$M_{t,p}$ - transverse moment - primary

$M_{t,s}$ - transverse moment - secondary

N_x - total longitudinal shear force

p' - plate load (net) per unit length

P_n - prestressing force in the n^{th} plate

$S_{n,n-1}$ - plate load at joint n, in the direction of joint n-1, per unit length

SU_n - sag constraint of n^{th} plate from upper limit

SL_n - sag constraint of n^{th} plate from lower limit

v_n - in-plane displacement of n^{th} plate

w_t' - component of gravity load in the plane of plate per unit length

x,y - plate coordinate directions

x_n - optimal value of prestressing force in n^{th} plate

y_n - optimal value of sag in n^{th} plate

$\sigma_{x,p}$ - longitudinal stress - primary

$\sigma_{x,s}$ - longitudinal stress - secondary

$\sigma_{x,n}$ - longitudinal stress at n^{th} ridge

$(\sigma_{xd})_n$ - longitudinal stress due to self weight, at n^{th} ridge

$(\sigma_{x\ell})_n$ - longitudinal stress due to live load, at n^{th} ridge

$(\sigma_{xw})_n$ - longitudinal stress due to wind load, at n^{th} ridge

$(\sigma_{xp})_{j,n}$ - longitudinal stress at n^{th} ridge, due to direct prestressing effect on j^{th} plate

$(\sigma_{xe})_{j,n}$ - longitudinal stress at n^{th} ridge, due to eccentric prestressing effect in j^{th} plate

ε_x - strain in x-direction

ε_y - strain in y-direction

τ - shearing stress

θ - angle which the algebraic maximum principal stress makes with x-axis

σ_1 - algebraic maximum principal stress

σ_2 - algebraic minimum principal stress

θ_{x0} - angle which the tangent to the prestressing cable at the end span makes with x-axis

Δ_{n0} - relative displacement between n^{th} and $n+1^{st}$ joints - secondary analysis

Ψ_{n0} - arbitrary rotation of n^{th} plate - secondary analysis

Ψ_n - actual rotation of n^{th} plate

ϕ_n - plate angle w.r.t. horizontal measured clockwise from the direction of the plate pointing towards the next plate

γ_n - plate deflection angle, measured clockwise from the extended direction of the plate to the direction of the next plate

μ - Poisson's Ratio

Chapter 1

INTRODUCTION

A folded plate structure is defined as a system of thin plates spanning longitudinally and monolithically joined to each other along longitudinal joints at some angle other than 180°. The structural behavior of folded plates is characterized by "slab" and "plate" actions. The loads acting normal to each plate cause it to bend transversely between the ridges as a continuous "slab". The plates supported at their ends on end-diaphragms, bend due to the in-plane "plate" loads. This behavior of the folded plate gives rise to longitudinal ridge stresses and transverse bending moments at ridges. With increasing spans, the longitudinal tension assumes very high values. This demands large quantities of steel resulting in an uneconomical design presenting problems in reinforcement congestion, splicing of steel, etc. These problems can be overcome by post-tensioning the folded plates which results in the following advantages:

1) Longitudinal tension is reduced with increasing span, thus saving steel.

2) The deflection of the structure is controlled.

3) A crackless structure which offers greater resistance to weathering agents becomes possible.

It may be stated that the object of prestressing is to place the folded plate into a pure membrane state.

Statement of the Problem

The objective of this thesis is to develop a method for analysis of prestressed folded plates and to determine the optimal selection of prestressing forces and cable locations. First, the tedious analysis of the folded plate will be carried out by computer and the output will give longitudinal ridge stresses, transverse ridge moments and principal stresses and their directions. The basic method of analysis will be that by Simpson (10). In order to check the computer program, examples already worked out by several authors will be carried out. The computer program will include the analysis for wind load in addition to prestressing and gravity loads. Analysis of folded plate for principal stresses and directions by Guralnick and Swartz (5) will be modified to incorporate the effect of prestressing. For any combination of loadings, a method for the selection of prestressing forces, cable sag and location, leading to an "optimal value" (minimum quantity of cable) will be developed. Folded plate analysis by beam theory will be compared with the Simpson method. The solution of prestressed folded plates using a finite difference method by Wayne Klaiber, Martin J. Gutzwiller and Robert H. Lee (12) will be compared with the method developed in this thesis. Finally, the validity of superposition will be checked.

Previous Work in This Area

Analysis and design of prestressed concrete folded plates has been carried out by John C. Brough and B. H. Stephens (3), treating the folded plate as a beam simply supported on end diaphragms. Analysis of prestressed folded plates by G. S. Ramaswamy (9) assumes the parabolic curve of the cable to be approximated by a sine curve. D. Yitzhaki (14) in his work suggests that shortening effects and bending effects due to prestressing be treated individually. But for different types of prestressing little work has been done to compute the longitudinal stresses and transverse moments, at different points along the longitudinal axis, treating the direct and eccentric effect of prestressing individually. Also, no one has suggested any systematic method to determine where, and how much prestressing should be applied to take care of various combinations of loadings. The general practice is a "trial and error approach" which may not, in most of the circumstances, lead to an optimum design. Also, no attempt has been made to check the validity of the superposition principle in the case of prestressing and other loads acting simultaneously.

Basic Assumptions

1) The material is elastic, homogeneous and uncracked.

2) The actual deflections are minor relative to plate width and length. Consequently, equilibrium conditions for a given plate may be developed using the configuration of undeflected plate.

3) The principle of superposition is valid. (This assumption will be checked later.)

4) The structure is monolithic and joints are rigid.

5) The length of each plate is more than twice its width.

6) In all plates plane sections remain plane after deformation. (It is, however, to be carefully noted that a plane cross section of the entire structure does not necessarily remain plane after deformation.)

7) Each supporting end diaphragm is infinitely stiff parallel to its own plane, but perfectly flexible, normal to its plane.

8) The strain is assumed to vary linearly across the width of each plate.

Chapter 2 contains a description of the method of analysis used and the development of a computer program to determine longitudinal ridge stresses, transverse ridge moments and principal stresses and their directions in folded plates. The computer program will analyze prismatic folded plates of any cross-section for gravity load, wind load and prestressing (parabolic draping or straight cable with or without eccentricity). The torsional stiffness of the edge beams is also included.

Chapter 3 contains several numerical examples.

Chapter 4 contains a comparison between the proposed method of analysis, and the beam method of analysis and the method of analysis using the finite difference solution of governing differential equations.

Chapter 5 describes a check on the validity of the principle of superposition.

Chapter 6 deals with the optimal selection of prestressing forces and cable sag. This chapter also includes several numerical examples.

Chapter 2

ANALYSIS OF FOLDED PLATES

2.1 Method of Analysis for Gravity Loads

Analysis of folded plates by H. Simpson (10) has been adopted for the development of the computer program. This is one of the methods recommended by the ASCE Task Committee (8).

Assumptions

1) In addition to the assumptions listed previously, the relative displacement Δ_n, between two adjacent joints, is assumed to vary sinusoidally along the longitudinal axis. If we denote Δ_{no} at midspan to be $(\Delta_{no})_c$,

$$\Delta_{no} = (\Delta_{no})_c \sin \frac{\pi x}{\ell}$$

where ℓ is the span and x is distance measured along the span from the end.

2) End plates are treated as cantilevers.

Outline of Method

Step 1 - Consider a transverse section of unit length at midspan of the given folded plate. Assuming that the joints do not deflect arrive at joint moments by moment distribution. Compute the reactions at joints and apply equal and opposite forces, V_n and H_n, at these joints. Resolve these applied forces into plate loads. Refer to Fig. 1 for force vector diagram. Compute the longitudinal bending stresses caused by the in-plane loads, $S_{n,n-1}$, etc., assuming the plates to be free to bend independently. These stresses are called free-edge stresses. Next, stress compatibility at the common edges is

THIS BOOK CONTAINS NUMEROUS PAGES WITH DIAGRAMS THAT ARE CROOKED COMPARED TO THE REST OF THE INFORMATION ON THE PAGE.

THIS IS AS RECEIVED FROM CUSTOMER.

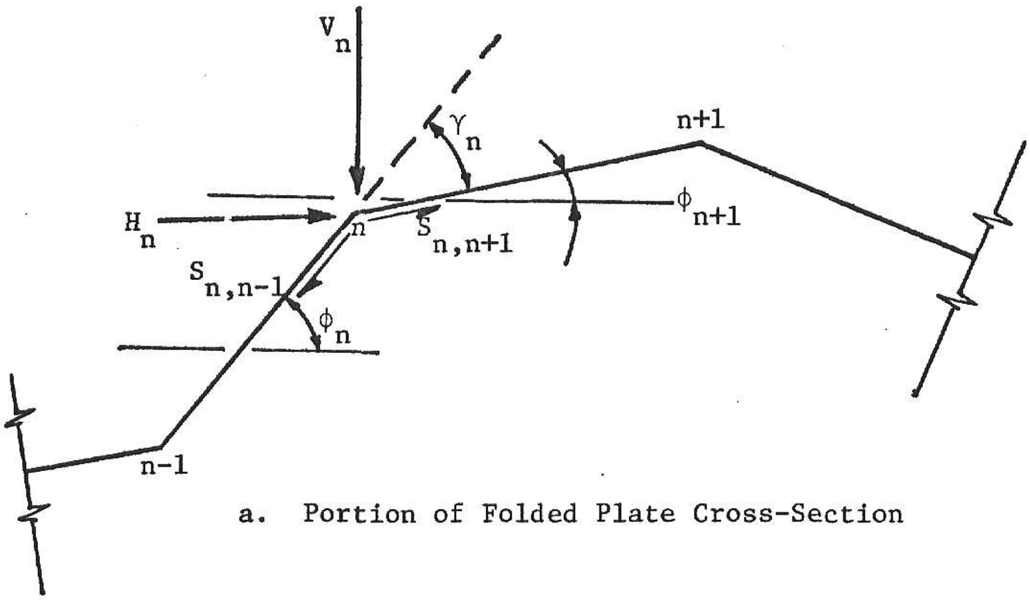

a. Portion of Folded Plate Cross-Section

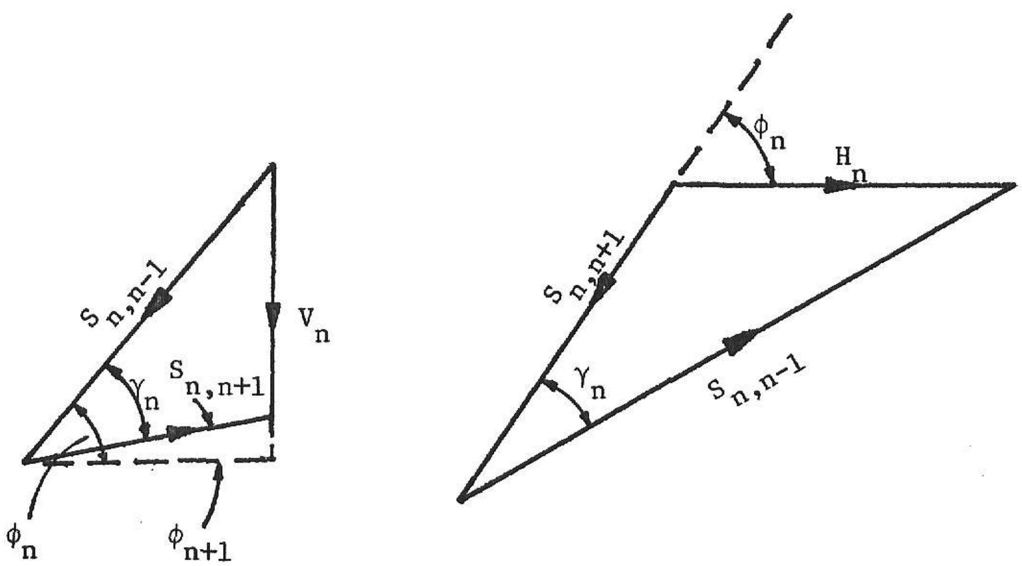

$S_{n,n-1} = V_n \text{ Cos } \phi_{n+1}/\text{Sin } \gamma_n$

$S_{n,n+1} = V_n \text{ Cos } \phi_n/\text{Sin } \gamma_n$

$S_{n,n-1} = H_n \text{ Sin } (\phi_n - \gamma_n)/\text{Sin } \gamma_n$

$S_{n,n+1} = H_n \text{ Sin } \phi_n/\text{Sin } \gamma_n$

b. Force Diagram at Joint n

Fig. 1 - Force Resolution at a Ridge of a Folded Plate

established by stress-distribution which is analogous to moment distribution. These final stresses are referred to as the primary solution.

Step 2 - The effects of relative joint displacements have now to be taken into account. Having treated the end plates as cantilevers, let joint 3 deflect by an arbitrary amount $\Delta 20$ below the level of joint 2, as shown in Fig. 2. The fixed end moment induced at joints 2 and 3 is $6EJ_2 \Delta_{20}/h_2^2$. Let the rotation of plate 2, Ψ_{20} be such that the magnitude of the moment induced is 6. Since $\Psi_{20} = \Delta_{20}/h_2$, then $\Psi_{20} = h_2/EJ_2$. The arbitrary rotation Ψ_{20} is related to the actual rotation Ψ_2 by, $\Psi_2 = K_2 \Psi_{20}$. These arbitrary moments at joints 2 and 3 are then distributed by moment distribution. Joint moments and reactions are found. Equal and opposite forces are applied at joints, resolved into plate loads, and free-edge stresses and hence, final edge stresses by stress distribution, are computed. This solution corresponds to the secondary solution due to arbitrary rotation of plate 2. Similarly, secondary solutions corresponding to arbitrary rotations of all plates except the first and last are found.

Step 3 - Now, expressions for primary and secondary plate deflections will be derived. (Refer to Fig. 3)

Primary Plate Deflection: Let $\sigma_{x,n}$ and $\sigma_{x,n+1}$ be the fiber stresses of the plate n at midspan. The plate moment at midspan, Mp_{max} is given by

$$Mp_{max} = \frac{1}{2} (\sigma_{x,n} - \sigma_{x,n+1}) d_n h_n \cdot h_n/6$$

where d_n is the thickness of the plate and h_n is the width of the plate.

$$Mp_{max} = \frac{1}{12} (\sigma_{x,n} - \sigma_{x,n+1}) d_n \cdot h_n^2 \text{ ---------------------- } (2.1)$$

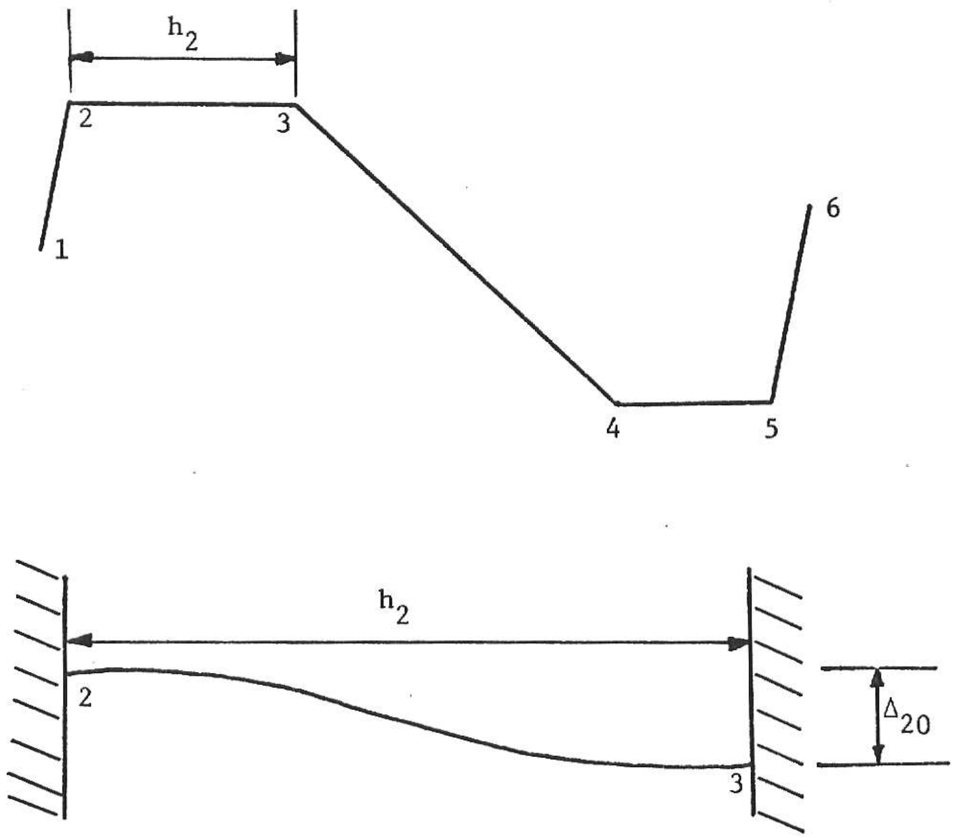

Fig. 2 - Structure Cross-Section Showing
Relative Joint Displacement

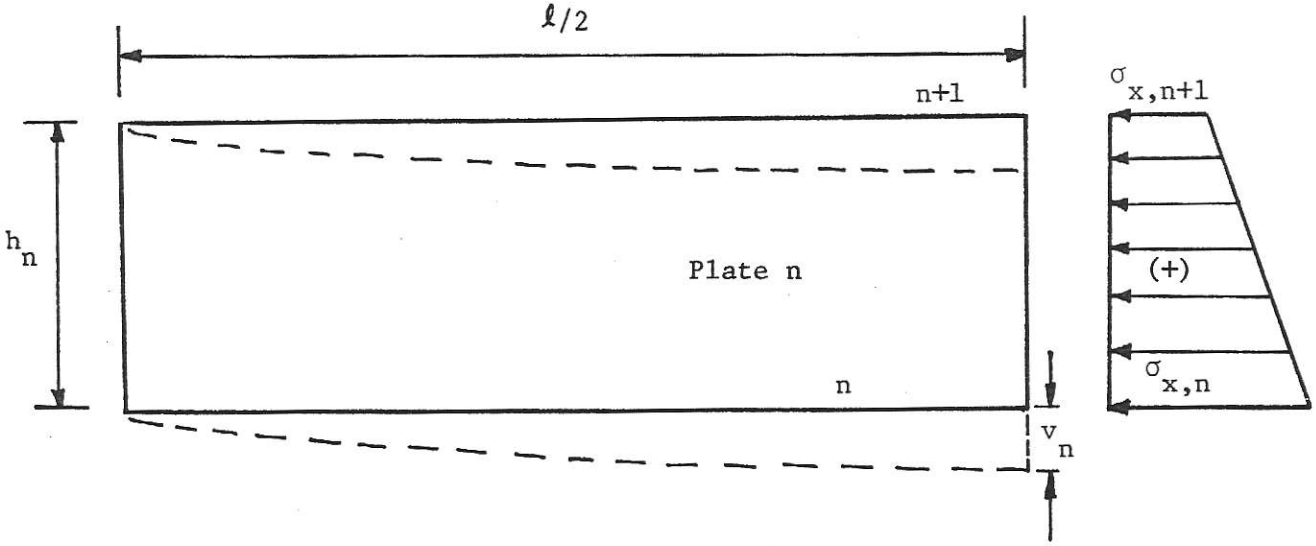

Fig. 3 - Distributed Plate Longitudinal Stresses and Deflections

The maximum plate moment Mp_{max} due to uniform plate load p' is given by

$$Mp_{max} = p'\ell^2/8 \quad \text{------------------------------------} \quad (2.2)$$

Equating (2.1) and (2.2) and knowing that the plate deflection at midspan due to uniform load p' is,

$$v_n = \frac{5}{384}\,(p'\ell^4/EJ_n), \text{ then}$$

$$v_n = \frac{5}{48}\,\frac{\ell^2}{Eh_n}\,(\sigma_{x,n} - \sigma_{x,n+1}) \quad \text{---------------------------} \quad (2.3)$$

Secondary Plate Deflection: The loading is proportional to the rotation, Ψ_{no}, of the plate, for which a sine variation along the span has been assumed. Two integrations of this loading will yield the bending moment at the center of the span which will be proportional to $\Psi_{no}\ (\ell^2/\pi^2)$.

$$Mp_{max} \propto \Psi_{no}\ \ell^2/\pi^2$$

Similarly, midspan deflection is proportional to $(\ell^4/\pi^4\ EJ_n)\Psi_{no}$. Hence, the deflection at midspan may be obtained by multiplying the bending moment at that section by $\ell^2/\pi^2\ EJ_n$. Also,

$$Mp_{max} = \frac{1}{12}\,(\sigma_{x,n} - \sigma_{x,n+1})\ d_n h_n^{\ 2}\ .$$

Hence, $$v_n = \frac{\ell^2}{\pi^2 Eh_n}\,(\sigma_{x,n} - \sigma_{x,n+1}) \quad \text{--------------------------} \quad (2.4)$$

Step 4 - From plate deflections v_n, plate rotations, Ψ_n can be computed. (Refer to Fig. 4 and Reference 9)

$$\Psi_n = \frac{1}{h_n}\left[v_{n+1}\,(\cot\gamma_n + \cot\gamma_{n-1}) - \frac{v_{n+2}}{\sin\gamma_n} - \frac{v_n}{\sin\gamma_{n-1}}\right] \text{--} \quad (2.5)$$

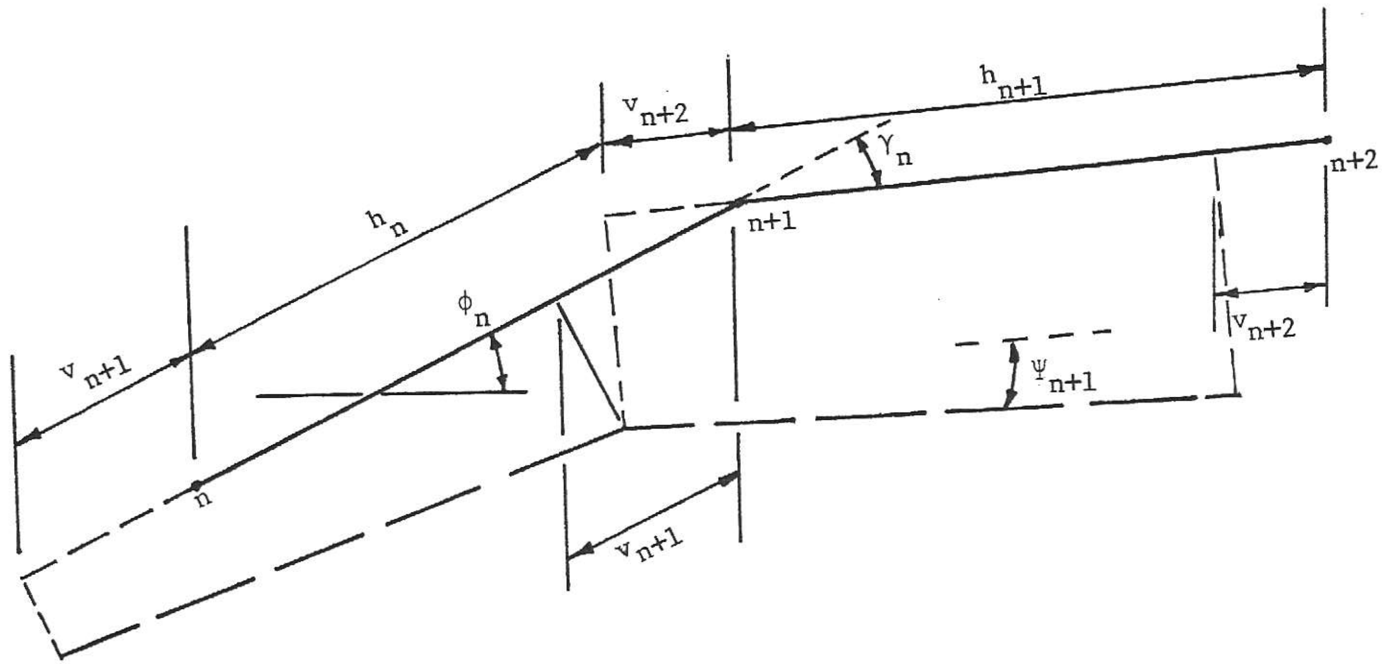

Fig. 4 - Portion of the Cross-Section of a Folded Plate Showing Position of Plates After Deformation

Also we know

$$\Psi_n = K_n \Psi_{no}, \text{ where } \Psi_{no} = h_n/EJ_n \quad \text{------} \quad (2.6)$$

From equations (2.5) and (2.6) we can calculate K_n (ie K_2, K_3...) solving (n-2) simultaneous equations.

Step 5 - The final solution of longitudinal stresses and transverse moments, at ridges, is computed by adding K_n times the secondary solution due to rotation of plate n, for all n-2 plates.

Variation of Longitudinal Stresses and Transverse Moments Along a Longitudinal Axis

Primary Solution: $\sigma_{x,p}$ varies parabolically and $M_{t,p}$ remains constant. If $\overline{\sigma}_{x,p}$ is the maximum σ_x at midspan for primary analysis,

$$\sigma_{x,p} = 4 \cdot \overline{\sigma}_{x,p} \cdot x\ (\ell - x)/\ell^2 \quad \text{------} \quad (2.7)$$

$$M_{t,p} = \text{constant}$$

where $\sigma_{x,p}$ and $M_{t,p}$ are longitudinal stress and transverse moment from primary analysis.

Secondary Solutions: If $\overline{\sigma}_{x,s}$ and $\overline{M}_{t,s}$ are maximum values at midspan,

$$\left.\begin{aligned} \sigma_{x,s} &= \overline{\sigma}_{x,s} \cdot \sin \frac{\pi x}{\ell} \\ M_{t,s} &= \overline{M}_{t,s} \cdot \sin \frac{\pi x}{\ell} \end{aligned}\right\} \quad \text{------} \quad (2.8)$$

where $\sigma_{x,s}$ and $M_{t,s}$ are longitudinal stress and transverse moment from secondary analysis.

The computation of principal stresses and their directions as developed by Guralnick and Swartz (9) is the basis for the computer program presented in this thesis.

2.2 Analysis for Wind Loading

Wind loading is essentially load normal to the plane of the plate. It will be a positive pressure on windward plates and negative (suction) pressure on leeward plates. A comprehensive study was made by an ASCE committee on wind forces and a final report was published in the ASCE transactions. It recommends that roofs of buildings be designed for varying pressures depending on their slope. Fig. 5, from Reference (2), gives the value of wind pressure as a function of the slope of the plate and whether it is on the windward or leeward side. These recommendations are based on an assumed wind velocity of about 78 m.p.h. with due allowances for suction and drag effects. The analysis for wind loads is the same as described previously for gravity loads.

2.3 Analysis for Prestressing

The method of analysis is same as that by Billington (1), except that the variation of longitudinal stress along the length of the span will be assumed to be constant as opposed to the sinusoidal variation assumed by Billington. Fig. 6 shows the in-plane load due to eccentric prestressing, and constant plate moment due to eccentric straight cable. The expression for the angle of inclination of the prestressing force with horizontal, at end span, (i.e.) θ_{xo}, can be derived as follows. Referring to Fig. 6.a,

$$e = 4 \cdot e_n \cdot x\,(\ell - x)/\ell^2$$

where e_n is the eccentricity at midspan and e is the eccentricity at a distance x from end.

$$\frac{de}{dx} = \frac{-8 \cdot e_n \cdot x}{\ell^2} + \frac{4 \cdot e_n}{\ell^2}$$

$$= 4 \cdot e_n \cdot (\ell - 2x)/\ell^2$$

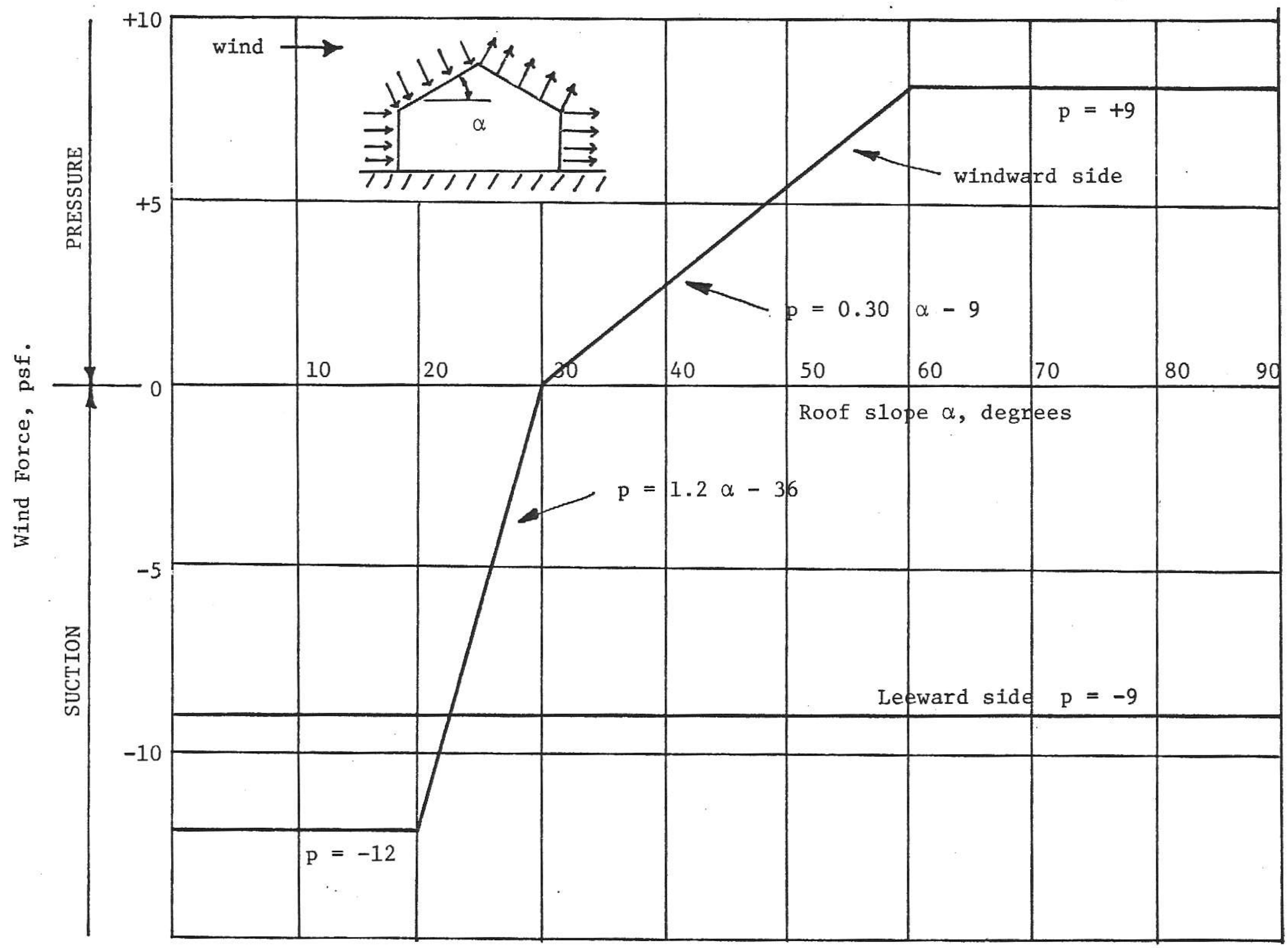

Fig. 5 - Wind Force on Buildings (ASCE Committee on Wind Forces)(2)

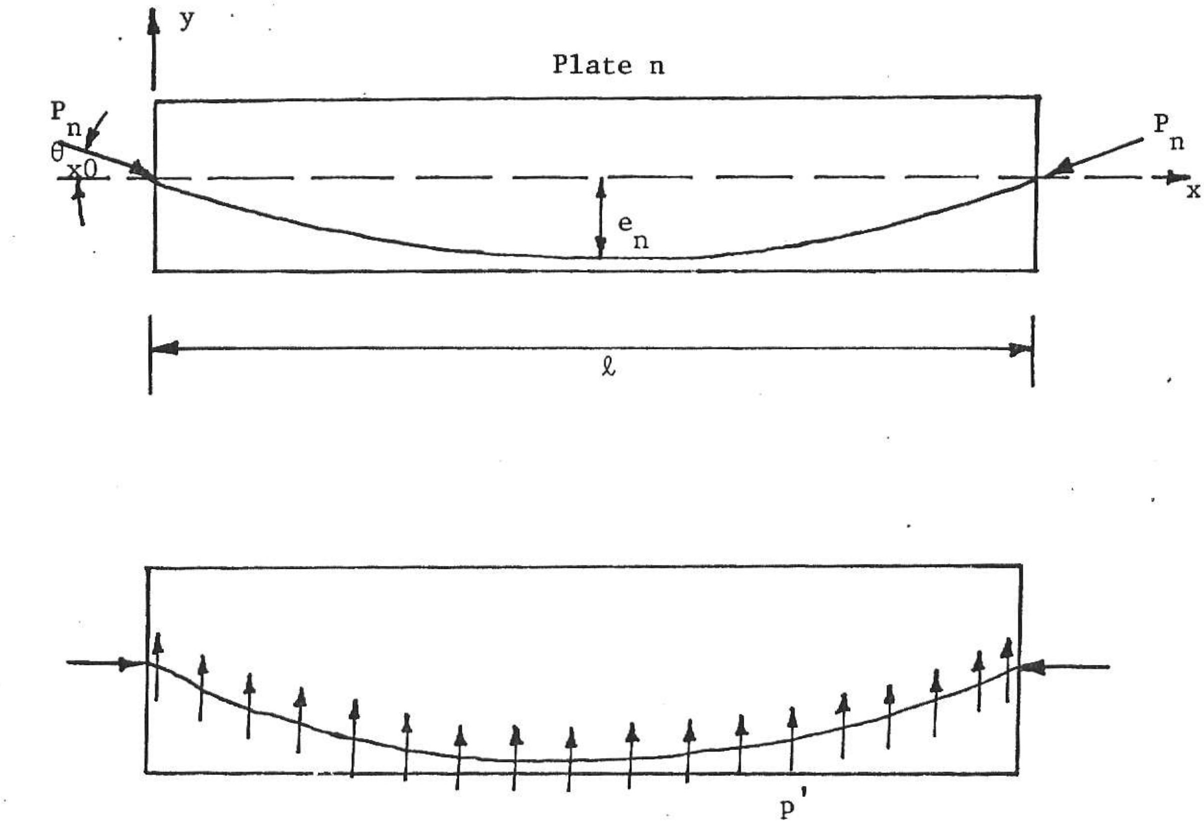

a. Parabolic Cable Profile

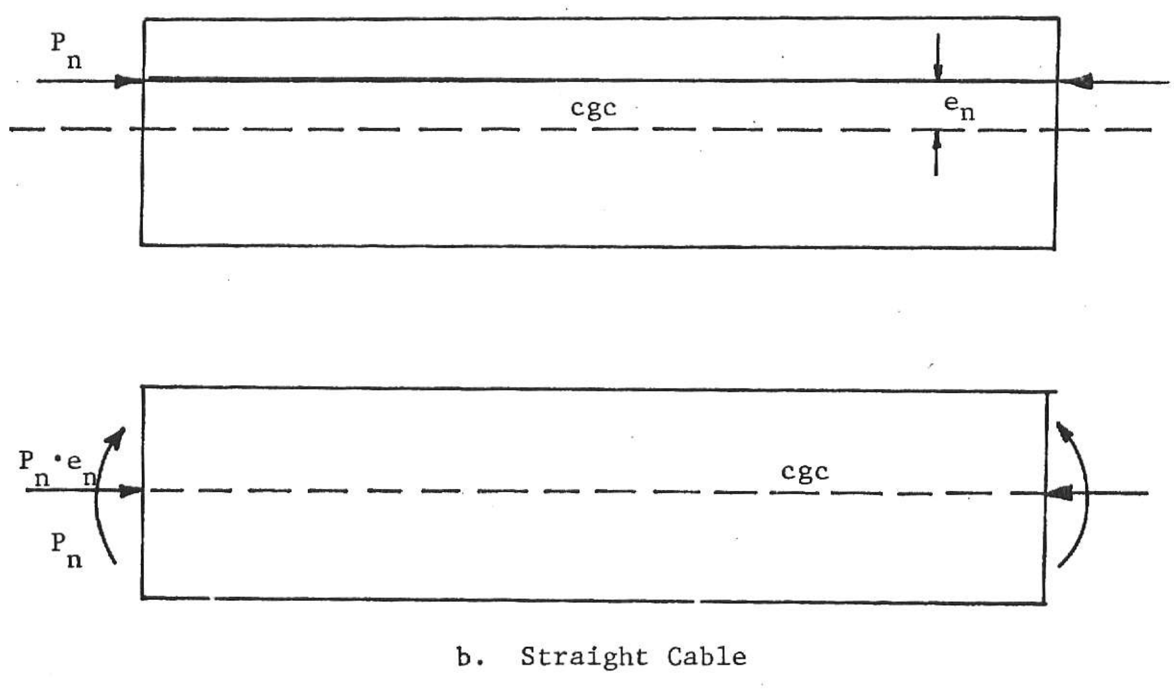

b. Straight Cable

Fig. 6 - Induced Plate Loads Due to Straight or Draped Prestressed Cables

$$\frac{de}{dx}\Big|_{x=0} = \tan \theta_{xo} = 4\ e_n/\ell$$

Hence, $\theta_{xo} = \tan^{-1} (4 \cdot e_n \cdot/\ell)$

and

horizontal component of prestressing force at end span =

$P_n \cdot \cos \theta_{xo}$

where P_n is the prestressing force, in nth plate.

The determination of stresses due to the in-plane loads caused by the draped cables follows the method given in Sec. 2.1. The direct forces due to prestressing create primary and secondary stresses which are also determined using the method described in Sec. 2.1.

2.4 Principal Stresses and Directions

Appendix A contains the method of calculation of principle stresses and directions for gravity loading, as developed by Guralnick and Swartz (5). Here a modification of this procedure to include prestressing effects is discussed.

The secondary solution for principal stresses is unchanged. However, the primary solution has to be modified. In addition to the parallel plate load from gravity loads, there will be a parallel plate load due to parabolic sag of the cable, given by 8 $P_n e_n/\ell^2$.

The method of analysis, once again is split into two, (i.e.):

1) The direct prestress, and

2) All other combinations of uniformly distributed loads including eccentric prestressing.

Since we know the longitudinal edge stresses (primary) corresponding to cases (1) and (2) individually, equilibrium equations can be written individually. In the case of direct prestress alone and considering the

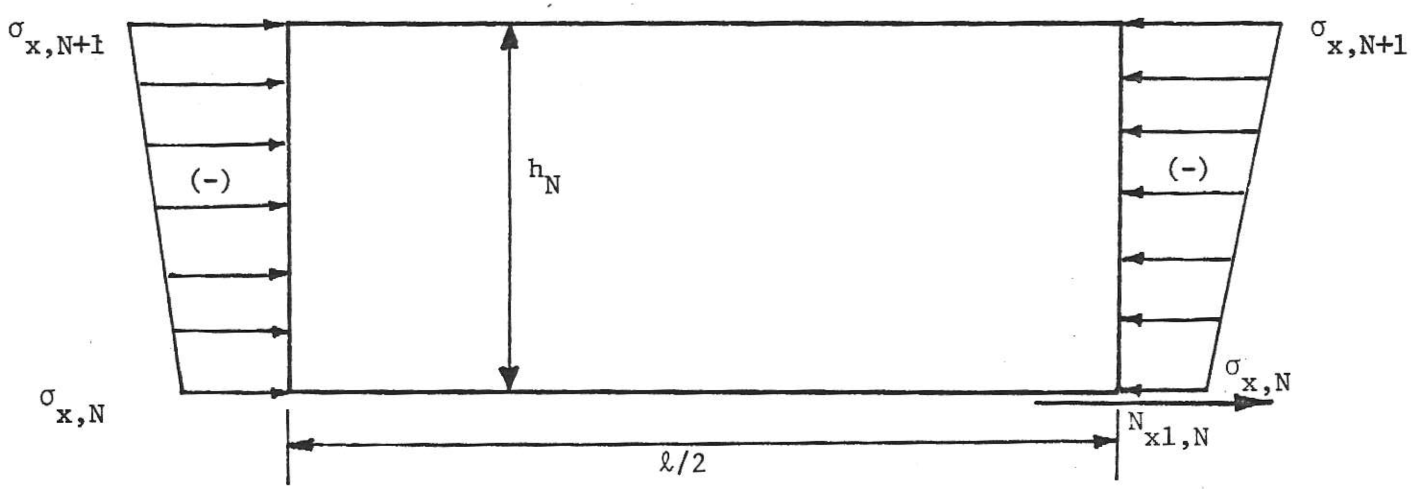

Fig. 7 - Primary Longitudinal Stresses in End Plate
Due to Direct Prestressing

equilibrium diagram, as shown in Fig. 7, the longitudinal stresses are constant along the length of the span and no edge shear force is produced at common ridges or elsewhere. That is,

$$N_{x\ (total)} = N_{x1} + N_{x2}$$

where N_{x1} = shear force due to direct prestressing alone

N_{x2} = shear force due to eccentric prestressing and other uniform loading

But, since $N_{x1} = 0$, then $N_{x\ (total)} = N_{x2}$

This point is to be kept in mind while deriving the normal stress and shearing stress equations; (i.e.) the values of longitudinal stresses used in these equations will not have those due to direct prestressing effect.

In the case of analysis for prestressing, the stress distribution close to the end spans will not be the same as the theoretical one. This is explained by St. Venant's principle. To obtain information about the distribution of stresses in the end-zones, one may refer to stress-distribution in end-block by Guyon (6). The actual stress distribution is quite complicated and beyond the scope of this thesis. But far from end spans the above analysis is found to be very much satisfactory. This will be proved later on when comparison with the finite difference method is carried out.

2.5 Torsional Stiffness of the Edge Beam

The edge beams, as shown in Fig. 8, can be treated as end plates in the analysis. But when the thickness of the beam is much greater than that of the adjacent plate, the torsional stiffness of the edge beam needs to be considered. Previously, the end plates were treated as

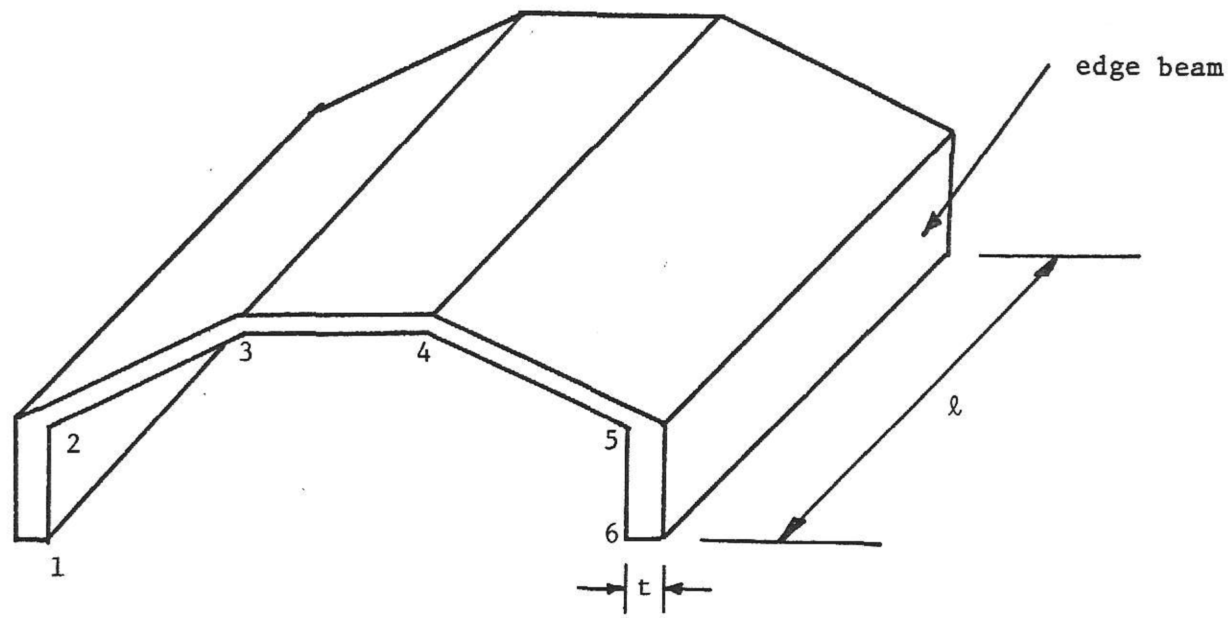

Fig. 8 - Folded Plate With Edge Beams

cantilevers. But in the case of edge beams it is necessary to compute the torsional stiffness of the edge beam in order to compute the distribution factors at joints 2 and N. Yitzhaki (14) has derived an expression for torsional stiffness of the beam which was consistent with his approximation of loading by a Fourier series expression in the case of the primary analysis. To be consistent with this primary analysis, it is necessary to find an expression for torsional stiffness of the edge beam which must be constant along its length, though actually it is not. The ACI Code Specification, as given in Reference 4 , indicates that torsional stiffness of a beam may be calculated by the expression

$$K_t = \frac{9E_{cs}c}{\ell \cdot (1 - c_2/\ell)^3}$$

where E_{cs} - modulus of elasticity of the slab concrete

c_2 - size of the wall, column bracket supporting the edge beam

c - pertains to the torsional rigidity of the edge beam, which for a rectangular cross section is given by Timoshenko, as in Appendix B.

$$c_2/\ell = 0$$

$$K_t \text{ edge beam} = \frac{9Ec}{\ell}$$

$$K_b \text{ adj. plate} = 4EKx\ell = \frac{4E\,d_n^{\,3}\ell}{12\,h_n}$$

$$\text{Distribution factor at joints 2 and N} = \frac{9Ec}{\ell} : \frac{4E\,d_n^{\,3}\ell}{12\,h_n}$$

$$= \frac{27c}{\ell^2} : \frac{d_n^{\,3}}{h_n}$$

2.6 Computer Program for the Analysis of Folded Plates

The computer program developed consists of a main program which computes the input to two subroutines. One subroutine carries out moment distribution and stress distribution and the output from it includes longitudinal ridge stresses and transverse ridge moments. The main program after obtaining the results from this subroutine computes necessary coefficients to determine the 'K' values which are then computed from the second subroutine which is a linear equation solver. The final longitudinal ridge stresses, transverse ridge moments and principal stresses and directions are computed in the main program.

The program operates in single precision. If the number of plates is greater than 8, it is recommended to run it in double precision.

The flow chart is given in the following section. The program source listing appears in Appendix C. Input-output details are given in Appendix D.

For any combination of loading, (dead load, live load, wind load and prestress) longitudinal ridge stresses and transverse ridge moments can be found at any section along the length of span. Also for any combination of loading, at any point in the folded plate, principal stresses and their directions can be determined. Flow charts are shown in Figs. 9 and 10.

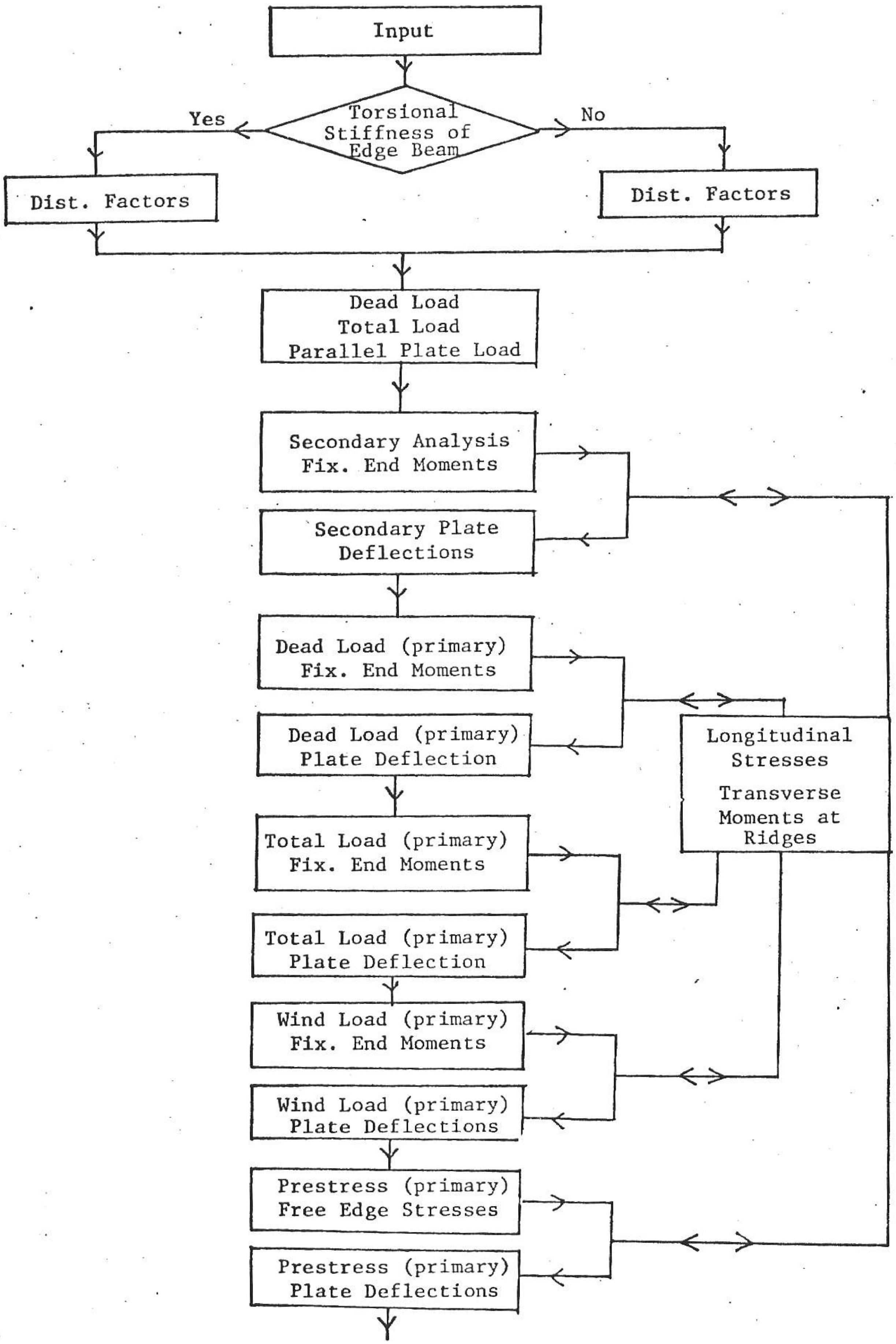

Fig. 9 - Flow Chart for General Folded Plate Analysis - Main Program